Generic critical points of normal matrix ensembles

Generic critical points of normal matrix ensembles

Razvan Teodorescu

Physics Department, Columbia University, 538 West 120th Street, Mail Code 5293, New York, NY 10027, USA

E-mail: rteodore@phys.columbia.edu

Abstract
The evolution of the degenerate complex curve associated with the ensemble at a generic critical point is related to the finite time singularities of Laplacian growth. It is shown that the scaling behaviour at a critical point of singular geometry $x^3 \sim y^2$ is described by the first Painlevé transcendent. The regularization of the curve resulting from discretization is discussed.

PACS numbers: 02.30.Ik, 02.50.Cw, 05.45.Yv, 47.15.Gp

1. Introduction

Random matrix theory, introduced to theoretical physics by Wigner and Dyson [1, 2] more than 60 years ago, has recently seen important new developments prompted by its application to several different problems. Of particular interest are generalizations to ensembles involving two independent matrices, such as 2-Hermitian random matrix theory (2HRM) and normal random matrix theory (NRMT). Rigorous results obtained in 2HRM over the last few years [3–9] have led to important relations concerning bi-orthogonal polynomials, the Riemann–Hilbert problem, and the Kadomtsev–Petviashvilii (KP) hierarchy of integrable differential equations. Results of similar nature have been obtained for normal matrix ensembles, sometimes with simple geometric interpretations [10–16], relevant to conformal maps in two dimensions [17–19].

Critical points of Hermitian random matrix ensembles have been studied intensively because of their important relations to 2D quantum gravity and string theory [20–25]; a similar analysis for generalized models of two matrices is under development. In NRMT, the evolution of the system towards the critical point has been given a clear hydrodynamic interpretation [10–16] in terms of the celebrated Hele–Shaw free-moving boundary problem [26–33]. In this paper, we continue this analysis and explore the scaling behaviour of the ensemble at a critical point.

Figure 1. The distribution of eigenvalues for the Gaussian potential. The droplet is an ellipse with quadrupole moment $2|t_2|$ and area $\pi\hbar N$.

2. Normal random matrix ensembles

2.1. Definitions

We briefly recall the basic concepts of NRMT [12, 34–36]: the object of study is the ensemble of $N \times N$ normal matrices M (i.e., which commute with their Hermitian conjugates, $[M, M^\dagger] = 0$), with statistical weight given by

$$\exp\left(\frac{1}{\hbar}\operatorname{tr} W(M, M^\dagger)\right) \mathrm{d}\mu(M), \tag{1}$$

and we choose for the present work the function W to be of the form

$$W = -|z|^2 + V(z) + \overline{V(z)}, \tag{2}$$

where $V(z)$ is a holomorphic function in a domain which includes the support of eigenvalues. In (1), $\hbar$ is an area parameter, and the measure of integration over normal matrices is induced by the flat metric on the space of all complex matrices. Upon integrating out angular degrees of freedom, the joint probability distribution of eigenvalues $z_1, \ldots, z_N$ is expressed as

$$\frac{1}{N!\tau_N}|\Delta_N(z)|^2 \prod_{j=1}^{N} \exp\left(\frac{1}{\hbar}W(z_j, \bar{z}_j)\right) \mathrm{d}^2 z_j. \tag{3}$$

Here $\mathrm{d}^2 z_j \equiv \mathrm{d}x_j\,\mathrm{d}y_j$ for $z_j = x_j + \mathrm{i}y_j$, $\Delta_N(z) = \det\left(z_j^{i-1}\right)_{1 \leqslant i, j \leqslant N} = \prod_{i > j}^{N}(z_i - z_j)$ is the Vandermonde determinant, and

$$\tau_N = \frac{1}{N!}\int |\Delta_N(z)|^2 \prod_{j=1}^{N} \exp\left(\frac{1}{\hbar}W(z_j, \bar{z}_j)\right) \mathrm{d}^2 z_j \tag{4}$$

is a normalization factor, the partition function of the matrix model.

2.2. Droplets of eigenvalues

It has been known for a long time that in a proper large N limit ($\hbar \to 0$, $t_0 = N\hbar$ fixed), the eigenvalues of M densely occupy a domain D in the complex plane. The first rigorous result was obtained by Ginibre [36] in the form of Circular law, later generalized by Girko to Elliptic law [37], illustrated in figure 1. In this case, the function $V(z)$ introduced in (2) is a quadratic polynomial, and the corresponding matrix model is referred to as Gaussian. Deformations of the droplet may be introduced by adding higher order terms to the function $V(z)$, provided they are small compared to the unperturbed potential, in a domain including the droplet [35]. In the region of validity, a power expansion of $V(z) = \sum_{k \geqslant 1} t_k z^k$ is expressed through the exterior harmonic moments of the droplet of eigenvalues (15) [14, 15].

2.3. Wavefunctions and complex orthogonal polynomials

In this section, we specify the potential (2) such that it properly defines a scalar product for analytic functions in the sense of Bargmann [38, 39]. The wavefunctions and orthogonal polynomials are defined through

$$\psi_n(z) = \exp\left(-\frac{|z|^2}{2\hbar}\right) \chi_n(z) \qquad \text{and} \qquad \chi_n(z) = \exp\left(\frac{1}{\hbar} V(z)\right) P_n(z), \tag{5}$$

where the holomorphic polynomials $P_n(z)$ are orthogonal in the complex plane with weight $e^{-[|z|^2 - 2\operatorname{Re} V(z)]/\hbar}$. They obey a set of differential equations with respect to the argument z, and recurrence relations with respect to the degree n. Multiplication by z may be represented on the basis of χ_n through a semi-infinite lower triangular matrix with one adjacent upper diagonal, $L_{nm} = 0$ for $m > n + 1$

$$L_{nm}\chi_m(z) = z\chi_n(z) \tag{6}$$

(summation over repeated indices is implied), and the differentiation ∂_z is represented by an upper triangular matrix with one adjacent lower diagonal. Integrating by parts the matrix elements of ∂_z, we have

$$(L^\dagger)_{nm}\chi_m = \hbar\partial_z\chi_n, \tag{7}$$

where $L^\dagger$ is the Hermitian conjugate operator.

Operators $L, L^\dagger$, may also be represented on the basis of the shift operator $\mathcal{W}$ defined through $\mathcal{W}\chi_n = \chi_{n+1}$, and become

$$L = R\mathcal{W} + \sum_{k\geqslant 0} U^{(k)}\mathcal{W}^{-k}, \qquad L^\dagger = \mathcal{W}^{-1}\bar{R} + \sum_{k\geqslant 0} \mathcal{W}^k \bar{U}^{(k)}, \tag{8}$$

where $R, U^{(k)}$ are diagonal semi-infinite matrices of elements $R_{nm} = r_n\delta_{nm}, U^{(k)}_{nm} = u^{(k)}_n\delta_{nm}, n, m \geqslant 0$ and δ_{nm} is the Kronecker symbol. Acting on χ_n, we obtain the commutation relation (the 'the string equation', compatibility of equations (6) and (7)):

$$[L^\dagger, L] = \hbar. \tag{9}$$

The string equation provides relations between the coefficients r_n and $u^{(k)}_n$. In particular, its diagonal part reads

$$n\hbar = r_n^2 - \sum_{k\geqslant 1}\sum_{p=1}^k \left|u^{(k)}_{n+p}\right|^2. \tag{10}$$

2.4. Example: normal Gaussian ensemble

For the case of Gaussian potential $V(z) = t_2 z^2, 2|t_2| < 1$, orthogonal polynomials P_n are given by complex Hermite polynomials of scaled variable [41]. Recurrence relations (8) become two-term
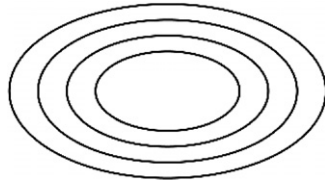
$$z\psi_n = r_n\psi_{n+1} + u_n\psi_{n-1}, \qquad (L^\dagger\psi)_n = r_{n-1}\psi_{n-1} + \bar{u}_{n+1}\psi_{n+1}, \tag{11}$$

and equations (9), (10) give the parameters r_n, u_n recursively through

$$2t_2 = \frac{\bar{u}_{n+1}}{r_n}, \qquad n\hbar = r_n^2 - |u_{n+1}|^2, \tag{12}$$

where the second equation is the area formula (10). Defining the two-component vector $\underline{\chi}_n = (\chi_{n-1}, \chi_n)^t$, we may express the action of the shift operator on $\underline{\chi}_n$ as

$$\mathcal{W}_n = \begin{pmatrix} 0 & 1 \\ -\dfrac{u_n}{r_n} & \dfrac{z}{r_n} \end{pmatrix}.$$

Figure 2. Growth in the non-critical Ginibre–Girko ensemble. The shape parameter of the ellipse $|t_2| < 1/2$, so the normalized area $t_0 = n\hbar$ may be increased indefinitely without encountering any singularity.

The operator $L^\dagger$ also acquires a reduced 2×2 matrix representation:

$$\mathcal{L}_n \underline{\chi}_{n+1} = \begin{pmatrix} z\dfrac{r_{n-1}}{u_n} & \bar{u}_{n+1} - \dfrac{r_n r_{n-1}}{u_n} \\ r_n - \dfrac{\bar{u}_{n+2} u_{n+1}}{r_{n+1}} & \dfrac{\bar{u}_{n+2}}{r_{n+1}} z \end{pmatrix} \underline{\chi}_{n+1}. \tag{13}$$

With the help of (12), $\mathcal{L}_n$ reads

$$\mathcal{L}_n(z) = \begin{pmatrix} z(2\bar{t}_2)^{-1} & -r_n(2\bar{t}_2)^{-1}(1 - 4|t_2|^2) \\ r_n(1 - 4|t_2|^2) & 2t_2 z \end{pmatrix}.$$

2.5. Complex curve

Since the operator $L^\dagger$ represents multiplication by $\bar{z}$, it is possible to define for each value of n a complex curve $f_n(z, \tilde{z}) = 0$ by solving the eigenvalue equation $\det[\mathcal{L}_n(z) - \tilde{z}] = 0$ and setting $\tilde{z} = \bar{z}$; we obtain an ellipse of equation

$$z\bar{z} - (t_2 z^2 + \bar{t}_2 \bar{z}^2)\frac{2}{1 + 4|t_2|^2} - n\hbar\frac{1 - 4|t_2|^2}{1 + 4|t_2|^2} = 0, \tag{14}$$

with the quadrupole moment $2|t_2|$ and area $\pi t_0 = \pi n \hbar$. This is precisely the boundary of the domain $\mathbb{D}_n$ filled by eigenvalues of the matrix model, at fixed $\hbar$, t_2 and n (or normalized area t_0).

The geometrical meaning of the complex curve (14) is straightforward: at fixed shape parameter t_2 and area parameter $\hbar$, increasing n yields elliptical domains that represent the support of the corresponding $n \times n$ Gaussian model. A remarkable feature of this process (represented in figure 2 and labelled *growth* in our previous works [14–16]) is that it preserves the external harmonic moments of the domain $\mathbb{D}_n$,

$$t_k(n) = t_k(n - 1), \qquad t_k(n) = -\frac{1}{\pi k} \int_{\mathbb{C}\backslash\mathbb{D}_n} \frac{\mathrm{d}^2 z}{z^k}, \quad k \geqslant 1. \tag{15}$$

The only harmonic moment which changes in this process is the normalized area $t_0 = \frac{1}{\pi} \int \mathrm{d}^2 z$, and it increases in increments of $\hbar$ (hence the meaning of $\hbar$ as quantum of area). We may say that the growth of the NRM ensemble consists of increasing the area of the domain by multiples of $\hbar$, while preserving all the other external harmonic moments. The continuum version of this process, known as *Laplacian growth*, is a famous problem of complex analysis. It arises in the two-dimensional hydrodynamics of two non-mixing fluids, one inviscid and the other viscous, upon neglecting the effects of surface tension (the Hele–Shaw problem [26–33]).

Figure 3. Deformation of the Gaussian ensemble and formation of boundary singularities.

2.6. Deformations and critical points of the ensemble

One of the most important properties of Laplacian growth is that, with the exception of special choices for the external harmonic moments t_k, the growth ends at a finite (critical) value of the area $t_0 = t_c$, when cusp-like singularities form on the boundary of the domain.

Laplacian growth of a simply-connected domain $\mathbb{D}(t_0)$ can be described [10–12] through a conformal map $z(w, t_0)$ which takes $\mathbb{C}\backslash\mathbb{B}_1$ into $\mathbb{C}\backslash\mathbb{D}(t_0)$, where $\mathbb{B}_1$ is the unit disk centred at the origin in the w-plane. Therefore, the conformal map has the form

$$z(w, t_0) = r(t_0)w + \sum_{k \geqslant 0} u_k(t_0)w^{-k}, \tag{16}$$

and the coefficients are functions of time (normalized area) t_0, such that

$$\{z(w, t_0), \bar{z}(w^{-1}, t_0)\} \overset{\text{def}}{=} w\left[\frac{\partial z}{\partial w}\frac{\partial \bar{z}}{\partial t_0} - \frac{\partial z}{\partial t_0}\frac{\partial \bar{z}}{\partial w}\right] = 1. \tag{17}$$

The Poisson bracket (17) encodes the infinite number of conservation laws

$$\frac{\mathrm{d}t_k}{\mathrm{d}t_0} = 0, \qquad t_k(t_0) = -\frac{1}{\pi k}\int_{\mathbb{C}\backslash\mathbb{D}(t_0)}\frac{\mathrm{d}^2z}{z^k}, \tag{18}$$

as well as the classical area formula

$$t_0 = r^2 - \sum_k k|u_k|^2.$$

As mentioned in the previous paragraph, we may regard Laplacian growth as the continuum limit of a corresponding NRM ensemble, sharing the same set of exterior harmonic moments. For instance, choosing the function $V(z)$ of the form

$$V(z) = \alpha \log\left(\frac{\beta}{\beta - z}\right) = \sum_{k \geqslant 1}\frac{\alpha}{k\beta^k}z^k, \qquad \text{Re}(\alpha) < 0, \tag{19}$$

corresponds to harmonic moments $t_k = \frac{\alpha}{k\beta^k}$ and the exterior of the droplet is given by the map [14]

$$z(w) = w\left[r + \frac{u}{a(w-a)}\right], \qquad |w| \geqslant 1, \tag{20}$$

where

$$\beta = \frac{r}{\bar{a}} + \frac{u}{a(1-|a|^2)}, \qquad t_0 = \bar{\alpha} + r^2 - \frac{ur}{a^2}. \tag{21}$$

For suitable values of α, the orthogonal polynomials corresponding to (19) are well defined, though they may obey complicated recurrence relations. In the continuum limit of the model, the droplet grows until its area reaches the critical value and a cusp forms on the boundary, figure 3. Formation of critical points is best described using the complex curve associated
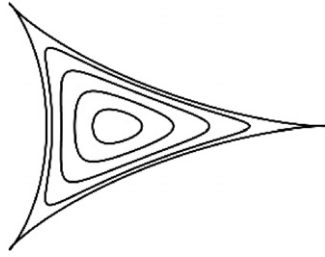
Figure 4. Critical points obtained from the cubic potential $V(z) = t_3 z^3$. Area of the droplet is increased at fixed t_3 until it reaches a maximal, critical value.

with the conformal map (20). As indicated in [14], it is a degenerate elliptic curve, with two branch points at $z_{1,2}$ inside the domain and a double point z_* outside. The critical point on the boundary appears when one of the branch points inside merges with the double point, leading to a cusp expressed in local coordinates as $x^3 \sim y^2$. Restoring finite values for n and $\hbar$ is equivalent to a discretization of the Laplacian growth and lifts the degeneracy of the complex curve of the continuum limit [15, 16].

2.7. Universality in the scaling region at critical points: a conjecture

Detailed analysis of critical Hermitian ensembles indicates that the behaviour of orthogonal polynomials in a specific region including the critical point (the *scaling region*), upon appropriate scaling of the degree n, is essentially independent of the bulk features of the ensemble. This *universality* property (a common working hypothesis in the physics of critical phenomena) is expected to occur for critical NRM ensembles as well—and is indeed easy to verify in critical Gaussian models, $2|t_2| = 1$. Analytically, it means that by suitable scaling of the variables z, n

$$n \to \infty, \qquad \hbar \to 0, \qquad n\hbar = t_0, \qquad t_0 = t_c - \hbar^\delta \nu, \qquad z = z_c + \hbar^\epsilon \zeta,$$

where z_c is the location of the critical point and t_c is the critical area, the wavefunction $\Psi_n(z)$ will reveal a universal part $\phi(\nu, \zeta)$ which depends exclusively on the local singular geometry $x^p \sim y^q$ (p, q mutual primes) of the complex curve at the critical point. This conjecture is a subject of active research. Its main consequence is that in order to describe the scaling behaviour for a certain choice of p, q, it is possible to replace a given ensemble with another which leads to the same type of critical point, though they may be very different at other length scales. More precisely, the scaling behaviour of operators in the vicinity of singular points illustrated in figure 3 is assumed to be identical to that of singular points in figure 4 (where $V(z) = t_3 z^3$), although the two critical droplets are obtained starting from different potentials. A constructive argument for this method is under development [42].

3. Scaling at critical points of normal matrix ensembles

In the remainder of the paper we analyse the regularization of Laplacian growth for a critical point of type $p = 3, q = 2$, by discretization of the conformal map as described in the previous section. For simplicity, we start from the conformal map corresponding to the potential $V(z) = t_3 z^3$, which is the simplest model leading to the specified type of cusp. It should be noted that the analysis will be identical for any monomial potential $V(z) = t_n z^n, n \geqslant 3$;
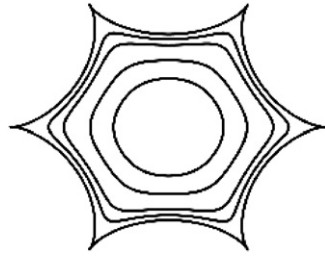
Figure 5. Critical boundary corresponding to $V(z) = t_6 z^6$.

for every such map, n singular points of type $p = 3$, $q = 2$ will form simultaneously on the boundary. The critical boundary corresponding to $n = 6$ is shown in figure 5.

3.1. Painlevé I as string equation

We start from the Lax pair corresponding to the potential $V(z) = t_3 z^3$ [14]:

$$L\psi_n = r_n\psi_{n+1} + u_n\psi_{n-2}, \qquad L^\dagger\psi_n = r_{n-1}\psi_{n-1} + \bar{u}_{n+2}\psi_{n+2}. \tag{22}$$

The string equation (9) $[L^\dagger, L] = \hbar$ translates into

$$\left(r_n^2 + |u|_n^2 - r_{n-1}^2 - |u|_{n+2}^2\right)\psi_n + (r_n\bar{u}_{n+3} - r_{n+2}\bar{u}_{n+2})\psi_{n+3}$$
$$+ (r_{n-3}u_n - r_{n-1}u_{n-1})\psi_{n-3} = \hbar\psi_n. \tag{23}$$

Identifying the coefficients gives

$$\left(r_n^2 - |u|_{n+2}^2 - |u|_{n+1}^2\right) - \left(r_{n-1}^2 - |u|_{n+1}^2 - |u|_n^2\right) = \hbar \tag{24}$$

and

$$\frac{\bar{u}_{n+2}}{r_n r_{n+1}} = \frac{\bar{u}_{n+3}}{r_{n+1}r_{n+2}} = 3t_3. \tag{25}$$

Equation (24) gives the quantum area formula

$$r_n^2 - \left(|u|_{n+2}^2 + |u|_{n+1}^2\right) = n\hbar, \tag{26}$$

which together with the conservation law (25) leads to the discrete Painlevé equation:

$$r_n^2\left[1 - 9|t_3|^2\left(r_{n-1}^2 + r_{n+1}^2\right)\right] = n\hbar. \tag{27}$$

In the continuum limit, the equation becomes

$$r^2 - 18|t_3|^2 r^4 = t_0. \tag{28}$$

The critical (maximal) area is given by

$$\frac{dt_0}{dr^2} = 0, \qquad 36|t_3|^2 r_c^2 = 1. \tag{29}$$

Choosing $r_c = 1$ gives $6|t_3| = 1$ and $t_c = \frac{1}{2}$. It also follows that:

$$u_n = \frac{r_{n-2}r_{n-1}}{2}, \qquad z_c = \frac{3}{2}. \tag{30}$$

Introduce the notation

$$N\hbar = t_c, \qquad n\hbar = t_0 = t_c + \hbar^{4a}v, \qquad r_n^2 = 1 - \hbar^{2a}u(v), \qquad z = \frac{3}{2} + \hbar^{2a}\zeta, \tag{31}$$

where $a = \frac{1}{5}$. We get $\partial_n = \hbar^a \partial_v$ and

$$r_{n+k}^2 = 1 - \hbar^{2a}u - k\hbar^{3a}\dot{u}(v) - \frac{k^2}{2}\hbar^{4a}\ddot{u}, \tag{32}$$

where dot signifies derivative with respect to v. The scaling limit of the quantum area formula becomes

$$(1 - \hbar^{2a}u)\left[\frac{1}{2} + \hbar^{2a}\frac{u}{2} + \hbar^{4a}\frac{\ddot{u}}{4}\right] = \frac{1}{2} + \hbar^{4a}v, \tag{33}$$

giving at order $\hbar^{4a}$ the Painlevé equation

$$\ddot{u} - 2u^2 = 4v. \tag{34}$$

Rescaling $u \to c_2 u$, $v \to c_1 v$ gives the standard form

$$\ddot{u} - 3u^2 = v, \tag{35}$$

for $c_2 = 4c_1^3$, $8c_1^5 = 3$.

3.2. Painlevé as compatibility equation

Use the modified wavefunctions (Pol represents the polynomial part)

$$\phi_n = \prod_{i=0}^{n-1} r_i \psi_n, \qquad \text{Pol } \phi_n(z) = z^n + O(z^{n-1}), \tag{36}$$

and rewrite the equations for the Lax pair as

$$L\phi_n = \phi_{n+1} + \frac{r_{n-2}^2 r_{n-1}^2}{2}\phi_{n-2}, \qquad L^\dagger \phi_n = r_{n-1}^2\phi_{n-1} + \frac{\phi_{n+2}}{2}. \tag{37}$$

Note that using the shift operator $\mathcal{W}$, the system can also be written as

$$L = \mathcal{W} + \frac{1}{2}\left(r_{n-1}^2 \mathcal{W}^{-1}\right)^2, \qquad L^\dagger = r_{n-1}^2 \mathcal{W}^{-1} + \frac{1}{2}\mathcal{W}^2. \tag{38}$$

Introduce the scaling function ψ through

$$\phi_n(z) = \exp\left(\frac{z^2}{2\hbar}\right)\psi(\zeta, v). \tag{39}$$

The action of Lax operators on ψ gives the representation

$$L = \frac{3}{2} + \hbar^{2a}\zeta, \qquad L^\dagger = z + \hbar\partial_\zeta = \frac{3}{2} + \hbar^{2a}\zeta + \hbar^{3a}\partial_\zeta. \tag{40}$$

Therefore, the action of ζ is given by the sum of equations at order $\hbar^{2a}$

$$3 + 2\hbar^{2a}\zeta = \mathcal{W} + \frac{1}{2}\mathcal{W}^2 + r_{n-1}^2\mathcal{W}^{-1} + \frac{1}{2}\left(r_{n-1}^2\mathcal{W}^{-1}\right)^2, \tag{41}$$

and the action of ∂_ζ by their difference:

$$\hbar^{3a}\partial_\zeta = -\mathcal{W} + \frac{1}{2}\mathcal{W}^2 + r_{n-1}^2\mathcal{W}^{-1} - \frac{1}{2}\left(r_{n-1}^2\mathcal{W}^{-1}\right)^2. \tag{42}$$

Equivalently, we can write

$$\hbar^{2a}\zeta = \frac{1}{2}\left[(\mathcal{W} + 1)^2 + \left(r_{n-1}^2\mathcal{W}^{-1} + 1\right)^2\right] - 4, \tag{43}$$

$$\hbar^{3a}\partial_\zeta = \frac{1}{2}\left[(\mathcal{W} - 1)^2 - \left(r_{n-1}^2\mathcal{W}^{-1} - 1\right)^2\right]. \tag{44}$$

Expanding the shift operator in $\hbar$ leads to

$$\mathcal{W} = 1 + \hbar^a \partial_v + \hbar^{2a}\frac{\partial_v^2}{2} + \hbar^{3a}\frac{\partial_v^3}{6}, \tag{45}$$

and

$$r_{n-1}^2 \mathcal{W}^{-1} = 1 - \hbar^a \partial_v + \hbar^{2a} \left(\frac{\partial_v^2}{2} - u \right) + \hbar^{3a} \left(-\frac{\partial_v^3}{6} + u \partial_v + \dot{u} \right). \tag{46}$$

Substituting into the equations for ζ, ∂_ζ gives the system of equations

$$\ddot{\psi} = \frac{2(\zeta + u)}{3} \psi, \qquad \psi' = \frac{\dot{u}}{6} \psi + \frac{2\zeta - u}{3} \dot{\psi}, \tag{47}$$

where primed variables are differentiated with respect to ζ. The equations can be written in matrix form as

$$\Psi' = \Lambda \Psi, \qquad \dot{\Psi} = Q \Psi, \qquad \Psi = \begin{pmatrix} \psi \\ \dot{\psi} \end{pmatrix}, \tag{48}$$

where

$$\Lambda = \begin{pmatrix} \dfrac{\dot{u}}{6} & \dfrac{2\zeta - u}{3} \\ \dfrac{\ddot{u}}{6} + \dfrac{2(\zeta + u)(2\zeta - u)}{9} & -\dfrac{\dot{u}}{6} \end{pmatrix}, \qquad Q = \begin{pmatrix} 0 & 1 \\ \dfrac{2(\zeta + u)}{3} & 0 \end{pmatrix}. \tag{49}$$

The compatibility equations

$$\dot{\Lambda} - Q' = [Q, \Lambda] \tag{50}$$

yield the Painlevé equation derived in the previous section

$$\dot{\Lambda} = \begin{pmatrix} \dfrac{\ddot{u}}{6} & -\dfrac{\dot{u}}{3} \\ \dfrac{\dddot{u}}{6} + \dfrac{2\zeta\dot{u} - 4u\dot{u}}{9} & -\dfrac{\ddot{u}}{6} \end{pmatrix}, \qquad Q' = \begin{pmatrix} 0 & 0 \\ \dfrac{2}{3} & 0 \end{pmatrix}, \tag{51}$$

and

$$[Q, \Lambda] = \begin{pmatrix} \dfrac{\ddot{u}}{6} & -\dfrac{\dot{u}}{3} \\ \dfrac{2(\zeta + u)\dot{u}}{9} & -\dfrac{\ddot{u}}{6} \end{pmatrix}. \tag{52}$$

Thus,

$$0 = \dot{\Lambda} - Q' - [Q, \Lambda] = \begin{pmatrix} 0 & 0 \\ \dfrac{\dddot{u}}{6} - \dfrac{6u\dot{u}}{9} - \dfrac{2}{3} & 0 \end{pmatrix}. \tag{53}$$

The only non-trivial element of the matrix gives

$$\dddot{u} - 4u\dot{u} - 4 = 0, \tag{54}$$

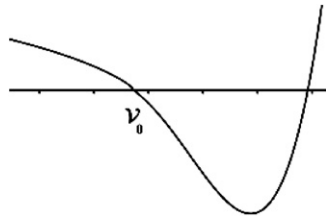i.e. the Painlevé equation derived in the previous section.

3.3. Painlevé and the non-degenerate spectral curve

In the scaling limit, the spectral curve is defined by the eigenvalue equation for the operator ∂_ζ,
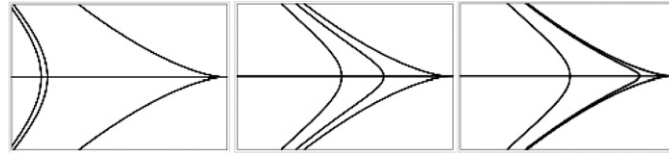
$$\partial_\zeta \Psi = \lambda(\zeta) \Psi, \tag{55}$$

or

$$\det[\lambda(\zeta) - \Lambda] = 0. \tag{56}$$

Figure 6. Physical solution for Painlevé I, with no singularities along the negative real axis.

Figure 7. Evolution of the non-degenerate curve (the leftmost boundary in each diagram) and degenerate curve (middle boundary) relative to the singular curve (right boundary), at (a) $v \to -\infty$, (b) $v_0 - v = O(1)$ and (c) $v_0 - v \ll v_0$.

We can write it also explicitly as an elliptic curve,

$$\lambda^2 = \left(\frac{2\zeta}{3} - \frac{u}{3} \right)^2 \left(\frac{2\zeta}{3} + \frac{2u}{3} \right) + \frac{2\zeta}{3} \cdot \frac{\ddot{u}}{6} + \frac{\dot{u}^2 - 2u\ddot{u}}{36}. \tag{57}$$

The critical points of the curve solve

$$\lambda_+ = \lambda_- = 0, \tag{58}$$

or

$$\mu^3 + \frac{2v}{3}\mu + \left[\left(\frac{\dot{u}}{6} \right)^2 - \frac{(u^2 + 6v)u}{27} \right] = 0, \tag{59}$$

where $\mu = 2\zeta/3$. Setting all derivatives to zero in (34) and (59), we get the degenerate solutions

$$\zeta_1 = -u = -\sqrt{-2v}, \qquad \zeta_{2,3} = \frac{u}{2} = \frac{\sqrt{-2v}}{2}. \tag{60}$$

We choose (up to exponential corrections) the solution to Painlevé I which is free of poles along the negative real axis, figure 6, and follow the evolution of the boundary as $t_0 \to t_c$, figure 7. As one can see, the presence of derivative terms lifts the degeneracy of the curve, so that the boundary remains smooth even as the area reaches its critical value.

(1) Quantum curve at $v \to -\infty$ In the case $v \to -\infty$, the asymptotic expansion of the solution to the Painlevé equation reads

$$u = \sqrt{-2v} - \frac{16}{v^2} + O(v^{-3}), \tag{61}$$

subject to exponential corrections. The curve becomes (figure 7, first diagram) non-degenerate, with simple critical points

$$\zeta_1 = -\sqrt{-2v} - \frac{1}{96v^2}, \qquad \zeta_{2,3} = \frac{\sqrt{-2v}}{2} + \frac{1}{192v^2} \pm \frac{i}{(-2v)^{3/4}}. \tag{62}$$

(2) Quantum curve at $u = 0$ Let $u(v_0) = 0$ define the smallest real solution of $u(v) = 0$. Then the local expansion reads

$$u(v) = \alpha(v - v_0) + 2v_0(v - v_0)^2 + \frac{2}{3}(v - v_0)^3 + \frac{\alpha^2}{6}(v - v_0)^4 + \cdots. \qquad (63)$$

Merging this regular expansion with the asymptote at $v \to -\infty$ yields

$$v_0 = -2^{\frac{7}{5}}, \qquad \alpha = \frac{1}{8v_0^3} + \frac{1}{\sqrt{-2v_0}} = -3 \times 2^{\frac{2}{5}}. \qquad (64)$$

The discriminant of (59) at $v = v_0$ becomes $\Delta^2 = \frac{9\alpha^4 + (8v_0)^3}{6^6} > 0$, so the equation has again one real solution and two complex conjugate roots. Moreover, since the free term is positive, it follows that the real solution is negative. The physical interpretation shows that the curve is smoothed out (figures 7(*b*) and (*c*)) at $u = 0$, instead of forming the classical (2, 3) cusp given by the degenerate curve.

Acknowledgments

References

[1] Wigner E P 1951 *Ann. Math.* **53** 36–67
[2] Dyson F 1962 *J. Math. Phys.* **3** 140–56
[3] Bertola M, Eynard B and Harnad J 2003 *Theor. Math. Phys.* **134** 27–38
[4] Bleher P and Its A 2002 *Preprint* math-ph/0201003
[5] Bertola M, Eynard B and Harnad J 2003 *J. Phys. A: Math. Gen.* **36** 3067–84
[6] Bertola M, Eynard B and Harnad J 2003 *Comm. Math. Phys.* **243** 193–240
[7] Kapaev A 2003 *J. Phys. A: Math. Gen.* **36** 4629–40
[8] Bleher P and Its A 2004 *Preprint* math-ph/0409082
[9] Bertola M, Eynard B and Harnad J 2004 *Preprint* nlin.SI/0410043
[10] Mineev-Weinstein M, Wiegmann P B and Zabrodin A 2000 *Phys. Rev. Lett.* **84** 5106
[11] Kostov I K, Krichever I, Mineev-Weinstein M, Wiegmann P B and Zabrodin A 2001 *MSRI* vol 40 (Cambridge: Cambridge University Press) p 285
[12] Wiegmann P B and Zabrodin A 2003 *J. Phys. A: Math. Gen.* **36** 3411–24
[13] Agam O, Bettelheim E, Wiegmann P B and Zabrodin A 2002 *Phys. Rev. Lett.* **88** 236802
[14] Teodorescu R, Bettelheim E, Agam O, Zabrodin A and Wiegmann P 2005 *Nucl. Phys.* B **704** 407
Teodorescu R, Bettelheim E, Agam O, Zabrodin A and Wiegmann P 2004 *Nucl. Phys.* B **700** 521
[15] Teodorescu R, Wiegmann P and Zabrodin A 2005 *Phys. Rev. Lett.* **95** 044502
[16] Bettelheim E, Wiegmann P and Zabrodin A 2005 *Preprint* nlin/0505027
[17] Wiegmann P B and Zabrodin A 2000 *Commun. Math. Phys.* **213** 523–38
[18] Marshakov A, Wiegmann P B and Zabrodin A 2002 *Comm. Math. Phys.* **227** 131–53
[19] Krichever I, Marshakov A and Zabrodin A 2003 *Preprint* hep-th/0309010
[20] Fokas A S, Its A R and Kitaev A 1992 *Commun. Math. Phys.* **147** 395–430
[21] David F 1993 *Phys. Lett.* B **302** 403–10
David F 1992 *Preprint* hep-th/9212106
[22] Di Francesco P, Ginsparg P and Zinn-Justin J 1995 *Phys. Rep.* **254** 1–133
[23] Chekhov L and Mironov A 2002 *Preprint* hep-th/0209085
[24] Kazakov V A and Marshakov A 2003 *J. Phys. A: Math. Gen.* **36** 3107–36
[25] Dijgraaf R and Vafa C 2002 *Preprints* hep-th/0208048, hep-th/0206255, hep-th/0207106, hep-th/0302011

[26] Hele-Shaw H S S 1898 *Nature* **58** no. 1489 34–36 520

[27] Galin L A 1945 *Dokl. Akad. Nauk SSSR* **47** 250–3

[28] Polubarinova-Kochina P Ya 1945 *Dokl. Akad. Nauk SSSR* **47** 254–7

[29] Kufarev P P 1947 *Dokl. Akad. Nauk SSSR* **57** 335–48

[30] Howison S, Lacey A and Ockendon J 1985 *Q. J. Mech. Appl. Math.* **38** 343

[31] Howison S 1986 *SIAM J. Appl. Math.* **46** 20

[32] Hohlov Y and Howison S 1993 *Q. Appl. Math.* **51** 777

[33] Bensimon D, Kadanoff L P, Liang S, Shraiman B I and Tang C 1986 *Rev. Mod. Phys.* **58** 977

[34] Chau L and Zaboronsky O 1998 *Commun. Math. Phys.* **196** 203–47

[35] Elbau P and Felder G 2004 *Preprint* math/0406604

[36] Ginibre J 1965 *J. Math. Phys.* **6** 440

[37] Girko V L 1986 *Theor. Probab. Appl.* **30** 677–90

[38] Bargmann V 1961 *Commun. Pure Appl. Math.* **14** 187–214

[39] Bargmann V 1962 *Proc. Nat. Acad. Sci. USA* **48** 199–204

[40] Orlov A Yu 2005 *Acta Appl. Math.* **86** 131–58

[41] Di Francesco P, Gaudin M, Itzykson C and Lesage P 1994 *Preprint* hep-th/9401163
     Akemann G 2002 *J. Phys. A: Math. Gen.* **36** 3363

[42] Teodorescu R Unpublished